



Dielectric and optical evaluation of high-emissivity coatings for temperature measurements in microwave applications

Beatriz García-Baños^{a,*}, Paolo Chiariotti^b, Rachele Napolitano^c, Giuseppe Pandarese^c, Laura Navarrete^d, Gian Marco Revel^c, Jose M. Catalá-Civera^a

^a ITACA Institute, Universitat Politècnica de València, Camino de Vera s/n, 46022 Valencia, Spain

^b Department of Mechanical Engineering, Politecnico di Milano, Via Giuseppe La Masa 1, 20156 Milano, Italy

^c Department of Industrial Engineering and Mathematical Sciences, Università Politecnica delle Marche, Via Brecce Bianche s/n, Ancona, (Italy)

^d Instituto de Tecnología Química, Universitat Politècnica de València—Consejo Superior de Investigaciones Científicas, Camino de Vera s/n, 46022 Valencia, Spain

ARTICLE INFO

Keywords:

High-emissivity coatings
High temperature
Microwave applications
Emissivity analysis
Chemical analysis
Dielectric properties

ABSTRACT

In this work, several commercial high-emissivity coatings have been characterized in terms of emissivity, chemical composition and dielectric properties as a function of temperature, under microwave irradiation. Accurate knowledge of their response under exposure to microwaves provides new and crucial information about their practical usability for non-contact temperature measurements in microwave environments. Due to their high metallic content, some of the studied coatings exhibited unexpected microwave-triggered reactions that hindered their use up to the maximum temperature specified by the manufacturers. Emissivity and chemical analyses before and after the heating cycles confirmed the degradation of some of the samples predicted by dielectric measurements. This work illustrates how a careful characterization of optical and dielectric properties under representative operating conditions (temperature range, microwave exposure) is vital in order to select the appropriate reference coating to obtain reliable temperature measurements in microwave applications.

1. Introduction

Microwaves are a clean and efficient form of energy with successful heating applications in many fields such as food processing, organic chemistry, plasma processing, sintering of metals, inorganic materials synthesis, etc. In all these applications, material temperature is one of the key variables providing indication on operating conditions, product quality and energy consumption status. Its real time measurement is also fundamental to avoid potential hazards in the reactors [1]. However, accurate temperature measurement inside a microwave applicator is a complex and nontrivial issue [2–4], especially in the case of high temperature microwave applications, with ranges covering from room temperature to more than 1000 °C during the process. The measurement devices should not perturb the microwaves, be affected by the electric and magnetic fields or modify the thermal distribution within the sample [5]. Therefore, from the multiple techniques for temperature measurements (thermocouples, pyrometers, temperature-sensitive paints, thermographic phosphors, etc.), non-contact Infrared (IR)

techniques are usually preferred in microwave processing applications [1,2,5,6].

The main advantages of non-contact IR thermal cameras are the possibility to measure in broad temperature ranges over an area (the effective Field of View – FoV – depends on the characteristics of the lens adopted) [2]. The camera detector calculates the temperature indirectly using the Stefan-Boltzmann law and the emissivity for the object of interest [2,7]; thus, accurate measurements require exact knowledge about the emissivity of the surface [6,8]. Inaccurate estimation of emissivity results in significant temperature errors: in high temperature applications, an error of 15–20% on the emissivity can lead to more than 200 °C deviations from the real temperature [4]. As emissivity is concerned, there are many factors affecting its value (spectral range, emission angle, surface geometry, just to cite some) hence its estimation is not trivial [9]. Different approaches have been proposed and developed for accurately characterize emissivity in wide temperature ranges: actually, they can be classified in direct (calorimetric or radiometric methods) and indirect (from reflectivity and transmissivity) approaches

* Corresponding author.

E-mail addresses: beagarba@upvnet.upv.es (B. García-Baños), paolo.chiariotti@polimi.it (P. Chiariotti), r.napolitano@staff.univpm.it (R. Napolitano), g.pandarese@staff.univpm.it (G. Pandarese), launaal@itq.upv.es (L. Navarrete), gm.revel@staff.univpm.it (G. Marco Revel), jmcatala@dcom.upv.es (J.M. Catalá-Civera).

<https://doi.org/10.1016/j.measurement.2022.111363>

Received 1 December 2021; Received in revised form 13 April 2022; Accepted 16 May 2022

Available online 19 May 2022

0263-2241/© 2022 The Authors. Published by Elsevier Ltd. This is an open access article under the CC BY-NC-ND license (<http://creativecommons.org/licenses/by-nc-nd/4.0/>).

[10,11]. The direct approach is targeted to high temperature and wide spectral ranges, while the indirect approach determines reflectivity (and consequently emissivity) in the near infrared (NIR) and visible (VIS) spectra, because of the higher radiation intensity at lower wavelengths ($<3\mu\text{m}$) at moderate temperatures [12]. The materials being processed in high-temperature processes undergo changing of their state during the process (e.g. changing from powder to agglomerates of different sizes) that cause a change in their emissivity. Tracking the evolution of their emissivity is therefore rather complex and results achievable might be subjected to wide uncertainty. Estimating the material temperature by monitoring the temperature of the material container through indirect approaches [13] seems to be a more robust method, as any uncertainty associated to the emissivity of the container can be reduced by exploiting high-emissivity coatings, as long as the coating withstands the process conditions [14,15]. The emissivity of such coatings should be known in the whole temperature range and be close to 1 (the ideal emissivity of a black body) in order to prevent reflection or radiation from surrounding heat sources. In the literature, references can be found providing the emissivity of paints that could be employed for accurate temperature measurements [2,5,14,16].

High-emissivity coatings entail other advantages, for which they are exploited with other multiple objectives: for energy savings [17–19], efficiency improvement of IR heaters [20,21], spacecraft thermal control [15,17] or as camouflage materials in defense technology [22,23]. From this latter application, it is well-known that high-emissivity coatings are typically characterized by effective microwave absorbance [22,23], due to their high content of metal powders (aluminum, zinc, stainless steel) [23–25]. Thus, the use of reference coatings inside a microwave environment can present some unexpected difficulties [4]. For example, recent studies reported that microwaves may lead to reactions occurring at significantly lower temperatures for certain metallic compounds [26], and in the case of reference coatings this could severely reduce their upper temperature limit.

Besides accurate determination of their emissivity, the use of reference coatings in microwave applications requires a good knowledge of their response under exposure to microwaves. Dielectric properties measurements determine their heating ability, being imperative to measure them under real operation conditions and in the expected temperature range of the application [2,27]. In the context of microwave absorbing materials for camouflage, typically the microwave reflection loss as a function of frequency is measured at room temperature [22]. However, reports containing high temperature dielectric characterization of materials under microwave conditions are scarce in the literature, and there are no previous studies on high-emissivity coatings.

In this work, several commercial high-emissivity coatings have been characterized in terms of emissivity, composition and dielectric properties measured as a function of temperature under microwave heating conditions. The effect of different factors affecting their performance as reference paints for high temperature measurements has been investigated. The results provide crucial information about their practical usability in microwave environments, with new constraints that need to be considered in these applications, so that engineers and metrologists can select the best option according to their specific application and ensure an appropriate performance of these coatings for accurate temperature determination.

2. Materials and methods

2.1. Materials

Five coatings from different manufacturers have been investigated. All coatings are high emissivity paints for temperature applications above $500\text{ }^\circ\text{C}$, with ingredients shown in Table 1.

The five coatings selected are quite different from each other in terms of temperature, composition and supplier. The rationale behind this

Table 1

Main characteristics of studied high-emissivity coatings.

Paint name	Maximum Temperature	Color	Supplier	Ingredients
HiE-Coat 840-CM	1093 °C	Black	AREMCO	Copper Chromite Black Spinel Magnesium Aluminum Silicate, Hydrated Mica Monoaluminum Phosphate Water
HiE-Coat 840-C	1093 °C	Black	AREMCO	Alumino-Silicate Copper Chromite Black Spinel Magnesium Silicate, Hydrated Silicon Dioxide, Amorphous Water
VHT-SPB102	1093 °C	Black	VHT	Acetone; Toluene; Propane; Butane Xylene, mixed isomers Pigment Black 26 (C.I. 77494) * Ethylbenzene Ethyl 3-Ethoxypropionate Amorphous Precipitated Silica Light Aliphatic Hydrocarbon
RUST-Oleum Heat Resistant Paint	750 °C	Black	Rawlins Paints	Hydrocarbons, C9-C11 n-/ iso-/ cyclo-alkanes, <2% aromatics Aluminum powder (stabilized) Phtalic anhydride Neodecanoic acid Cobalt salt
TERMOTIX	650 °C	Silver	TIXE	Silicone resin Selected thermoresistant pigments

* Pigment Black 26 (C.I. 77494) is a black mixed oxide of Manganese (II) and Iron (III) with chemical formula MnFe_2O_4 and a spinel structure.

choice is to demonstrate that the market offers several options to tackle the issue of delivering high-emissivity coatings for high-temperature applications. Nevertheless, despite all of them might promise excellent performance, it is important to clearly understand their pros and cons, in order to select the coating that truly and robustly satisfies the requirements of the experiment one is looking to conduct. In fact, performance stability is a key driver for selecting the proper coating at both the experiment design and running levels. The paper is exploring the coatings with the clear intent of identifying the one best-performing in a particular application, i.e. high-temperature MW-based heat treatments.

2.2. Methods

Specimens of the different coatings were cured according to the procedures given by the manufacturers: (i) HiE-Coat 840-CM was air-dried at room temperature for 1 h, then heated for 30 min at $95\text{ }^\circ\text{C}$ and 1 h at $260\text{ }^\circ\text{C}$; (ii) curing of HiE-Coat 840-C was accomplished by air-drying at room temperature for 1 h, then heating for 1 h at $95\text{ }^\circ\text{C}$; (iii) curing of VHT-SPB102 was accomplished by air-drying at room temperature for 1 h; then heating for 30 min at $120\text{ }^\circ\text{C}$, cooling for 30 min, and reheating for 30 min at $200\text{ }^\circ\text{C}$; (iv) curing of RUST-Oleum was accomplished by air-drying at room temperature for 3 h, then heating at $150\text{ }^\circ\text{C}$ in stages of $50\text{ }^\circ\text{C}/\text{hour}$; (v) curing of TERMOTIX was accomplished by air-drying at room temperature for 1 h and then heating for 1

h at 200°.

Once the coatings were cured, they were studied in terms of microwave and IR optical related performance by several analysis techniques described below.

2.2.1. Dielectric properties as a function of temperature

The behavior of a dielectric material under the application of an electromagnetic field is determined by its permittivity. It is a complex number whose real part (or dielectric constant) represents the ability of the material to be polarized by the applied electric field and store energy, and the imaginary part (or loss factor) represents its ability to transform this energy into heat. The permittivity is greatly influenced by the material chemical composition and temperature, but also important differences have been evidenced in the permittivity of microwave-heated samples respect to those conventionally heated [28]. Thus, in order to reproduce the exact conditions of application, the permittivity of samples was measured at different temperatures under microwave heating conditions.

The microwave setup (Figure S1) consisted of a dual-mode cylindrical cavity operating simultaneously with two independent microwave signals, one for heating the specimen (max. power 150 W) and another one to measure the permittivity (max. power 1mW) [29]. Both subsystems worked simultaneously on the sample, but the different electromagnetic modes employed (TE₁₁₁ and TM₀₁₀) and a cross coupling filter avoided any interference between them. Each specimen was placed in a quartz tube (filling a cylindrical volume of 9.8 mm diameter, 15 mm height), and inserted in the cavity through a hole equipped with a filter to avoid any microwave leakage. A PID algorithm adjusted the microwave source to heat the specimen at a constant heating rate of 15 °C/min. The temperature of the specimen was measured with a IR pyrometer through a hole in the lateral wall of the cavity. The bulk temperature of the specimen was determined from quartz holder surface measurements through a careful calibration procedure described in [30]. The methodology to obtain the permittivity of the sample as a function of the temperature was based on the shift of the resonance frequency and the change of the quality factor of the cavity in the presence of the sample as compared to the empty cavity [29]. The accuracy of this method was estimated to be 3% for the dielectric constant and 10% for the loss factor in the whole temperature range.

2.2.2. XRD analysis

The effect of microwave heating on the composition of the different paints was studied by X-ray Diffraction (XRD) in a PANalytical Cubix fast diffractometer by using CuK α 1,2 radiation, and an X'Celerator detector. XRD patterns were recorded in the 2 θ range from 20 to 90° and analyzed using the X'Pert HighScore Plus software. For that purpose, specimens before and after microwave treatment were grinded with a porcelain mortar and pestle and characterized by XRD, allowing the crystalline phases identification.

2.2.3. Emissivity temperature dependency analysis (Radiometric Method)

The temperature dependency of each specimen's emissivity was assessed at high temperatures by comparing the thermal radiation emitted at given temperatures by the specimen under test and a reference coating (see Figure S2 for more details on the experimental set-up). Indeed, if the two coatings are tested simultaneously on the same target, equivalence of temperatures of the coatings can be assumed, hence the unknown emissivity of a coating can be calculated from the Stefan-Boltzmann law of grey body as follows:

$$\epsilon_{coat,u} = \epsilon_{coat,ref} \frac{W_{coat,u}}{W_{coat,ref}} \quad (1)$$

where W is the total power per unit area radiated from an object, ϵ is the emissivity and the subscripts *coat,ref* and *coat,u* refer to the reference and tested coating respectively.

The specimen HiE-Coat 840-C coating was selected to serve as a

reference, given the availability of emissivity values at different temperatures. The coating was applied by a sponge brush on a half side of four ceramic holders (one for each investigated specimen) with surface properly free of oil, grease, dirt, corrosives, oxides, paints or other contaminants and cured following the procedure described in section 2.2. The other coatings tested were applied on the other side of the tiles, close to the reference one, and cured as addressed in their technical specifications.

Each ceramic holder was heated in a conventional electric kiln from temperature ambient up to 900 °C by alternating forced heating (kiln door open) and natural cooling phases (due to the opening of the front door to perform IR measurements). The surface temperature was measured by an Infratec IR camera ($\lambda = 7.5\text{--}14 \mu\text{m}$) every 100 °C interval for 5 min (one point per 30 s) once the kiln was turned off (Figure S2, A). A type-K thermocouple was attached on the front side of the specimen holder, to monitor continuously (one acquisition point per second) its temperature (Figure S2, B). Data related to target heating temperature of 100 °C were not considered in the analysis, because the narrower temperature difference with the environment prevented to have repeatable results.

2.2.4. Spectral emissivity in UV-Vis-NIR range

The spectral emissivity of specimens was determined in UV-Vis-NIR range ($\lambda = 0.3\text{--}2.5 \mu\text{m}$) with a spectrophotometer (Jasco V-670) at ambient temperature, (Figure S3). The total reflectivity spectrum of each specimen was estimated by using a 150 mm diameter Integrating Sphere. The spectral emissivity was obtained from the Kirchhoff's law for opaque specimens, assuming that the incident radiation transmitted is 0 [12]:

$$\epsilon(\lambda) = 1 - R(\lambda) \quad (2)$$

where: $\epsilon(\lambda)$ is the spectral emissivity, $R(\lambda)$ is the spectral reflectivity, λ is the wavelength.

A comparison between the spectral emissivity before and after heating was also performed, with the aim to analyse the preservation status of each paint subjected to the maximum declared heating temperature.

3. Results

3.1. Dielectric properties

Fig. 1 presents the dielectric properties (dielectric constant and loss factor) of all the specimens measured during microwave heating and free cooling cycle, always below the maximum operation temperature specified by the manufacturer in each case (Table 1).

In the case of HiE-Coat-840-C (Fig. 1.a)), dielectric properties showed a smooth increase with temperature. The loss factor was medium at room temperature (0.03 at 23 °C) and between 400 and 500 °C the specimen presented a change in the slope, indicating an increasing capacity to absorb microwave energy, up to moderate values of loss factor at the maximum temperature (0.73 at 1050 °C). This change in the loss factor led to a higher heating rate from 400 °C (inset in Fig. 1). The initial dielectric properties were measured after the free cooling of the sample, proving the reversibility of the process. Dielectric measurements showed that this material presents moderate microwave absorption, but high stability during the heating cycle, without abrupt reactions taking place, and also without important modifications of its properties after the microwave treatment.

Similar dielectric properties were obtained for the specimen HiE-Coat-840-CM (Fig. 1.b)) but an abrupt increase was observed in this case at temperatures above 900 °C. From this temperature, moderate values of the loss factor (1.8 at 1030 °C) indicated reactions or transformations in the material leading to a greater capacity of the material to absorb microwave energy. However, the sample remained stable in terms of dielectric properties after the microwave treatment, as shown

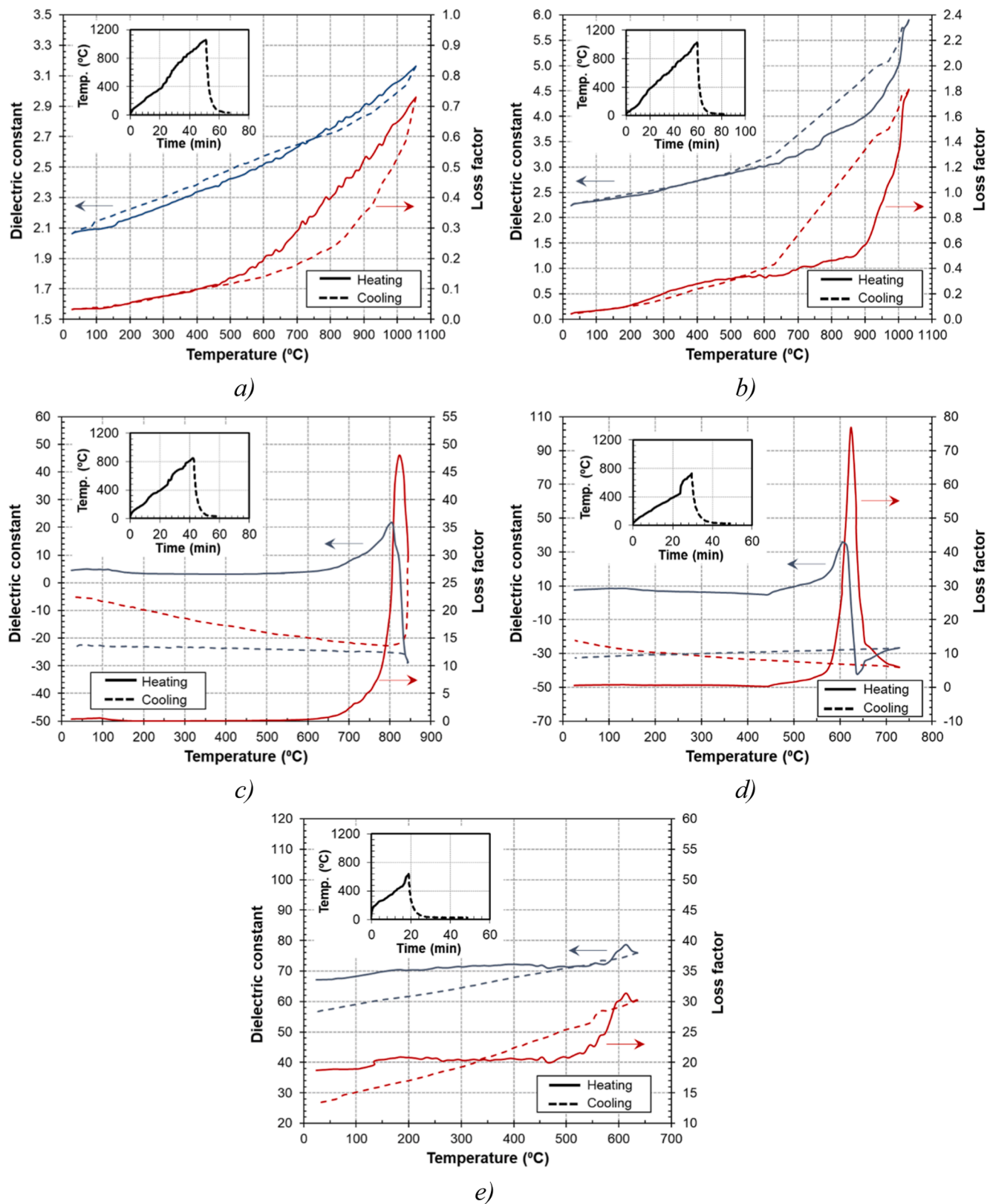


Fig. 1. Dielectric properties of studied coatings during microwave heating and cooling cycles. Insets: Evolution of specimen temperature during the test. (a) HiE-Coat-840-C, (b) HiE-Coat-840-CM, (c) VHT-SPB102, (d) RUST, (e) TERMOTIX.

by the dielectric values obtained after the cooling cycle. In this case, the information revealed by dielectric measurements indicates that this sample is not so stable as the previous one, since the abrupt increase of microwave absorption capacity from 900 °C could possibly lead to

thermal runaway when used at higher temperatures. Nevertheless, the reversibility showed by dielectric properties indicates that this sample maintains the main properties after the heating cycle, and a good performance could be expected under microwave heating conditions.

The coating VHT-SPB102 (Fig. 1.c) presented higher capacity to absorb microwave energy than previous specimens (loss factor 0.4 at 23 °C), with a very notable and abrupt increase from 700 °C, reaching high values of both loss factor (43 at 823 °C) and dielectric constant (22 at 807 °C). These maxima indicated that reactions or transformations in

the sample were leading to a higher capacity of the material to be polarized and convert microwave energy into heat, due to a higher mobility of free charges, ions or dipoles. The behavior of the curves from approx. 820 °C indicated that metallic components began to dominate, and thus the assumption that the material is pure dielectric was not valid

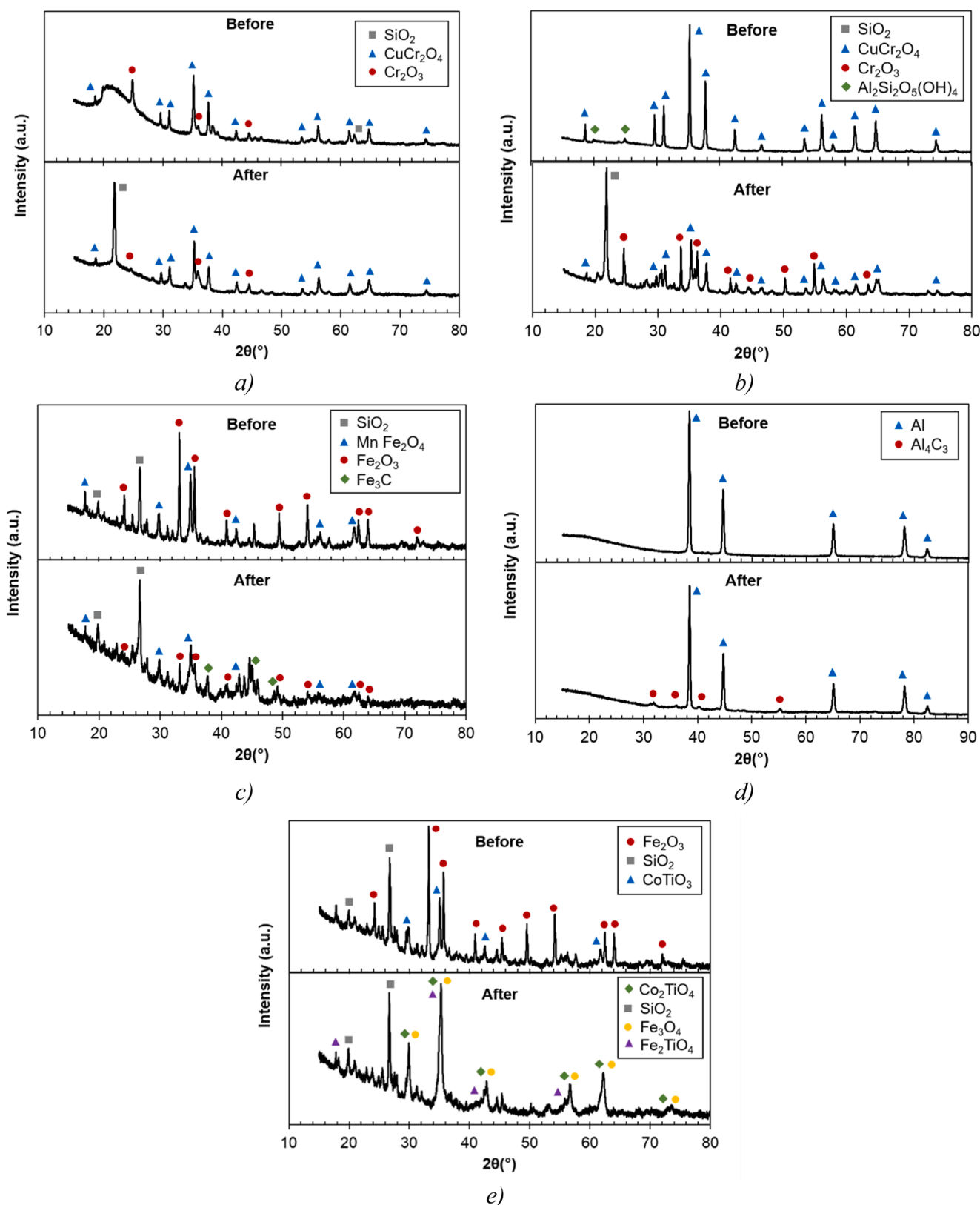


Fig. 2. XRD analysis of coatings before and after the microwave heating cycle. (a) HiE-Coat-840-C, (b) HiE-Coat-840-CM, (c) VHT-SPB102, (d) RUST, (e) TERMOTIX.

anymore. The metallic behavior of this sample was also evidenced by small arcs and sparks that were visible in the specimen from 450 to 500 °C, which could be also explained by its iron content (Table 1). This fact did not allow heating the material closer to the maximum temperature specified by the manufacturer (1093 °C).

Similar dielectric properties and behavior were observed for RUST-Oleum specimen (Fig. 1.d)). It had moderate loss factor at room temperature (0.5 at 23 °C) which remained almost constant up to 450 °C, where a reaction started increasing the microwave absorption and accelerating the heating rate from 15 to 17 °C/min to 37–40 °C/min. As in previous case, measured dielectric values indicated a predominant metallic behavior from 600 °C to the maximum temperature of the experiment (730 °C), fixed below the maximum of 750 °C specified by the manufacturer. Substantial changes were observed in the dielectric values after the cooling cycle, proving irreversible changes in the material after microwave heating.

In Fig. 1 (e) shows the dielectric properties of TERMOTIX specimen as a function of temperature, with high initial values of both dielectric constant (67 at 23 °C) and loss factor (18.7 at 23 °C) due to a high metallic content, which led to the apparition of small arcs and sparks especially above 450 °C. From this temperature, the capacity of the material to absorb microwaves was even increased by a reaction in the sample that accelerated the heating rate to 54 °C/min. Although maximum temperature was 636 °C, below the maximum temperature specified by the manufacturer (650 °C), irreversible changes occurred in the material as illustrated by the dielectric values obtained after the cooling cycle.

In Fig. 1(c), (d) and (e), dielectric properties revealed a new constraint affecting the practical usability of these coatings in microwave applications, since unexpected microwave-triggered reactions took place at temperatures well below the maximum temperatures specified by the manufacturer, leading to important and irreversible changes in the material dielectric properties. As reported in previous studies with similar materials [26], these reactions can occur at lower temperatures than those observed under conventional heating. Thus, dielectric properties measurement provided new information about the temperature limits that should apply to this material in practical microwave applications.

3.2. XRD analysis

Fig. 2 illustrates the XRD analysis of each specimen before and after the microwave treatment (*hkl* index are provided in figure S4). In the case of HiE-Coat-840-C (Fig. 2.a)), the initial specimen perfectly matched the information provided by the manufacturer (Table 1) and the main difference observed in the treated sample was that amorphous SiO₂ sinterized to a cristobalite structure, but the rest of components such as the copper chromite black spinel remained unchanged after the microwave heating cycle, as expected from the dielectric properties results. Similar composition was observed for HiE-Coat-840-CM specimen (Fig. 2.b)) except for the absence of amorphous SiO₂, as indicated by the manufacturer in Table 1. After microwave treatment, the sample showed the formation of chrome oxide, with the concomitant reduction of copper chromite black spinel intensity and the formation of SiO₂ at the expense of magnesium aluminum silicate reduction.

Metallic behavior observed during microwave heating of specimen VHT-SPB102 was evidenced in the XRD analysis (Fig. 2.c)) due to the iron content specified by the manufacturer (Table 1). Irreversible changes revealed by the dielectric properties after the heating cycle matched the changes in the XRD analysis of the heated specimen, with several iron oxides and the formation of cementite (iron carbide).

XRD analysis of RUST-Oleum (Fig. 2.d)) showed the aluminum as the main component, as expected from the information in Table 1. After the microwave treatment, the formation of aluminum carbide was observed, which, according to dielectric analysis, seems to have notable implications on the material capacity to be polarized by microwave fields. This

could be expected since carbides are, in general, good microwave absorbers (for example, silicon carbide is a well-known material employed as microwave susceptor in microwave applications).

XRD analysis of TERMOTIX specimen (Fig. 2.e)) showed typical iron oxides employed as black pigments. Different reactions between the components occurred during the microwave cycle, as evidenced by the XRD results after the treatment, leading to the irreversible changes previously observed in the dielectric properties.

3.3. Emissivity as a function of temperature

In the case of emissivity determination, the final temperature of the heating process was set to 900 °C, but the analysis was performed only on the temperature ranges that could be effectively investigated by the use of the IR camera. Since this was possible only by opening the front door of the kiln and by shutting down its heating system (to prevent non-repeatable heating phenomena driven by the kiln control system), cooling of the specimens occurred. This is clear if looking at the temperature data measured by the thermocouples on the ceramic holders during the thermal camera measurements (Fig. 3). It can be seen how temperature decreases while the kiln front door is open. It is interesting also to observe that temperature data are consistent and repeatable during the four tests performed on the four coatings. The time-shift that is evident on the test related to VHT-SPB102, indeed does not affect the temperature values reached during that test, which is consistent to those measured in the other tests. Temperature data were collected with the thermal camera for 5 min after shutting down the kiln and opening its front door. The last acquisition point (after 5 min) of each cooling phase was used in the emissivity analysis, as it was experimentally found to be the most stable one. A detailed explanation of this procedure can be found in the Supporting Information (Figures S5–S7). Moreover, to avoid providing emissivity values at different temperature values for each coating (given the slight natural variability of the final temperature at the end of each cooling phase), once the emissivity values were calculated at the actual temperatures exploiting equation (1), they were interpolated (4th degree polynomial) at those temperatures in which reference emissivity data were available for the Hi-Coat 840-C.

To verify the robustness of the whole approach, the emissivity values of HiE-Coat 840-CM and HiE-Coat 840-C specimens were measured and compared to those provided by the manufacturer (Table 2), using each of them alternatively as reference. It is well evident the consistency of emissivity values obtained by the procedure exploited, given the full compatibility (data lying within the uncertainty boundaries) with data

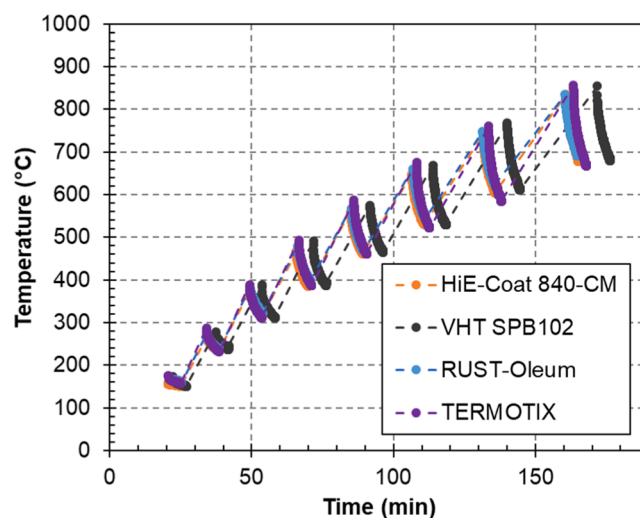


Fig. 3. Thermocouples temperature profiles in the intermediate temperature range (200–900 °C).

Table 2

Estimated total emissivity of HiE-Coat 840-CM and HiE-Coat 840-C from radiometric measurements and comparison with the available theoretical values from datasheet.

T (°C)	HiE-Coat 840-CM (datasheet)	HiE-Coat 840-CM (calculated) ^a	HiE-Coat 840-C (datasheet)	HiE-Coat 840-C (calculated) ^b
300	0.94 ± 0.02	0.93	0.89 ± 0.02	0.89
400	0.95 ± 0.02	0.94	0.89 ± 0.02	0.88
500	0.95 ± 0.02	0.94	0.88 ± 0.02	0.88
600	0.94 ± 0.04	0.93	0.88 ± 0.03	0.88
700	0.94 ± 0.04	0.92	0.88 ± 0.03	0.89

^a HiE-Coat 840-C used as reference.

^b HiE-Coat 840-CM used as reference.

reported in the coatings datasheet.

Table 3 reports the total emissivity values of all the specimens analysed at the investigated temperatures. The emissivity values of reference specimen HiE-Coat-840-C provided by the manufacturer are also included for comparison purposes. All the specimens showed emissivity values above 0.9, thus confirming their high-emissivity nature. Data of the TERMOTIX coating are reported just up to 500 °C as this is the temperature corresponding to the heating step towards 600 °C (TERMOTIX maximum operating temperature is 650 °C, hence data above this threshold would not be reliable). HiE-Coat 840-CM and VHT-SPB102 shows very similar emissivity values. The RUST-Oleum seems to be the one ensuring the highest emissivity. However, its limited temperature range would prevent its use in demanding high-temperature applications (e.g. higher than 1000 °C).

3.4. Spectral emissivity

Fig. 4 shows the spectral emissivity of the specimens before and after heating. Assessing the stability of the specimens in these conditions is fundamental to ensure the possibility of re-using the target coated with the high-emissivity painting once it undergoes a heat treatment.

Before heating, all specimens show high total emissivity values (around 0.92) in the VIS range ($\lambda = 0.3 - 0.6 \mu\text{m}$) of the whole Vis-NIR spectrum investigated ($\lambda = 0.3 - 2.5 \mu\text{m}$). The specimen RUST-Oleum presents the most stable spectral emissivity at room temperature in the whole Vis-NIR range. The specimens HiE-Coat 840-CM and HiE-Coat 840-C are characterized by a spectral emissivity ranging from 0.8 (at $\lambda \sim 1.0 \mu\text{m}$ and $\lambda \sim 1.5 \mu\text{m}$) to 0.98 (λ greater than $2 \mu\text{m}$). Both the VHT-SPB102 and the TERMOTIX specimens are characterized by a total spectral emissivity decaying around $\lambda \sim 0.9 \mu\text{m}$. This preliminary characterization would suggest the possibility of exploiting RUST-Oleum, HiE-Coat 840-CM and HiE-Coat 840-C also with non-contact measurement systems (e.g. pyrometers, etc.) working in the NIR range, as their spectral emissivity is high enough (higher than 0.8) over the whole investigated spectrum. However, the post-heating characterization adds interesting information regarding the possibility to re-use

Table 3

Total emissivity values at different temperatures for HiE-Coat 840-C (datasheet values) and for the coatings tested by radiometric measurements.

T (°C)	HiE-Coat 840-C	HiE-Coat 840-CM	VHT-SPB102	RUST-Oleum	TERMOTIX
300	0.89 ± 0.02	0.93	0.92	0.95	0.91
400	0.89 ± 0.02	0.94	0.93	0.96	0.93
500	0.88 ± 0.02	0.94	0.94	0.96	0.95
600	0.88 ± 0.03	0.93	0.93	0.96	-
700	0.88 ± 0.03	0.92	0.93	0.95	-

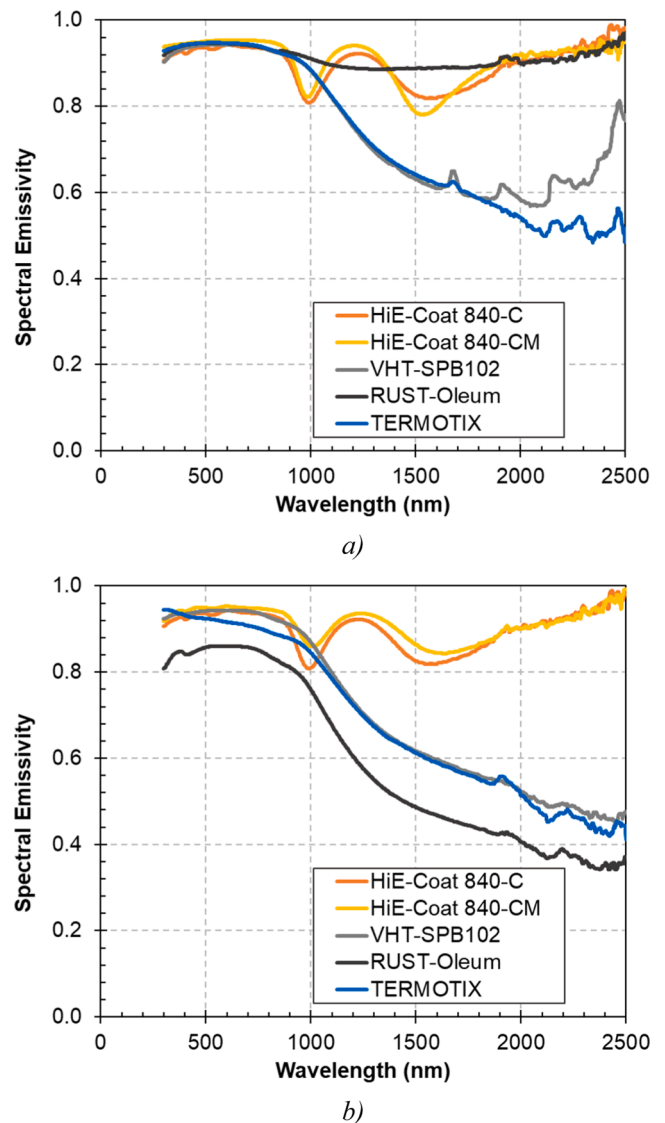


Fig. 4. Total spectral emissivity values from spectrophotometric measurements, (a) before and (b) after heating.

the coated target once it undergoes the heating process. Indeed, specimens HiE-Coat 840-CM and HiE-Coat 840-C show very small variations of the spectral emissivity in the recorded Vis-NIR range ($\lambda = 0.3 - 2.5 \mu\text{m}$). TERMOTIX and VHT-SPB102 specimens have a very similar emissive behavior in the Vis-NIR range, before and after heating. In particular, VHT-SPB102 shows small change of the spectral emissivity in the NIR range (from 1.5 to $2.5 \mu\text{m}$) after reaching the maximum heating temperature. RUST-Oleum also presents a significant change of the spectral emissivity after heating, in this case in the Vis-NIR range.

Visual analysis of the samples before/after heating (see Figure S8) made it possible to conclude that HiE-Coat 840-CM, HiE-Coat 840-C and VHT coatings remain well adherent to the holder without any detachment. Deterioration of the coating surface was to be reported for the TERMOTIX and RUST-Oleum specimens. A slight colour, as highlighted by the spectral emissivity data, is observed on RUST-Oleum.

It should be noted here that those samples showing variations in their spectral emissivity after the heating cycle (RUST-Oleum, TERMOTIX, VHT) were those also showing variations in their dielectric properties. This fact suggests the possibility to exploit dielectric characterization (with few-minutes tests) as a fast and convenient tool to predict changes in the emissivity performance after the heating cycle, as previously proved for other similar sensing applications [26].

3.5. Summary of results

Two of the samples (HiE-Coat 840-CM and HiE-Coat 840-C) presented medium to moderate microwave absorption, but high stability under high temperature microwave heating, in terms of chemical composition, emissivity and dielectric properties.

The high metallic content commonly present in high emissivity coatings lead to some of the specimens (VHT-SPB102, TERMOTIX) having undesired interactions with microwave fields with small arcs or sparks that could hinder accurate determination of surface temperature. In practical applications, the surrounding atmosphere (gases being prone to be ionized) could further promote these problems and even lead to plasma ignition.

Dielectric properties also showed that some of the samples (VHT-SPB102, RUST-Oleum) underwent unexpected chemical reactions, promoted at lower temperatures by an enhanced mobility of dipoles or charges due to the presence of the microwave field, as supported by previous studies in the literature [26,28]. This fact would not impede but limit their use at temperatures below the maximum operating temperature specified by the manufacturers. This temperature limitation is also motivated by the degradation (visual changes, color alteration) or detachment observed in some of the samples (RUST-Oleum, TERMOTIX).

Finally, some of the studied samples (VHT-SPB102, RUST-Oleum, TERMOTIX) presented a change in their emissivity in certain spectral ranges after the heating cycle being this of importance if these coatings are to be employed as references to obtain accurate temperature measurements in practical applications.

4. Conclusion

This work combined in situ dielectric characterization of several coatings under microwave heating with measurements of their spectral emissivity before and after the heating cycle. The results from the different analyses allowed the evaluation of these coatings to be used as references for temperature measurements in high temperature microwave applications.

Unexpected results demonstrated that a careful characterization of optical and dielectric properties under representative operating conditions (microwave heating, high temperature) is crucial to select the appropriate reference coating. The fact that industrial microwave applications are increasingly becoming more popular due to their economic and environmental benefits could also prompt the manufacturers to develop specific coatings with adapted features to improve their performance as temperature references.

Funding.

This research was funded by the European Union's Horizon 2020 research and innovation programme under grant agreement number 820783.

CRediT authorship contribution statement

Beatriz García-Baños: Conceptualization, Writing – original draft. **Paolo Chiariotti:** Methodology, Investigation, Writing – review & editing. **Rachele Napolitano:** Data curation, Formal analysis. **Giuseppe Pandarese:** Software, Investigation. **Laura Navarrete:** Investigation, Formal analysis. **Gian Marco Revel:** Resources, Supervision. **Jose M. Catalá-Civera:** Resources, Writing – review & editing.

Declaration of Competing Interest

The authors declare that they have no known competing financial interests or personal relationships that could have appeared to influence the work reported in this paper.

Appendix A. Supplementary material

Supplementary data to this article can be found online at <https://doi.org/10.1016/j.measurement.2022.111363>.

References

- [1] D. Pan, Z. Jiang, Z. Chen, W. Gui, Y. Xie, C. Yang, Temperature measurement method for blast furnace molten iron based on infrared thermography and temperature reduction model, *Sensors* 18 (2018) 3792, <https://doi.org/10.3390/s18113792>.
- [2] L. Gangurde, G. Sturm, T. Devadiga, A. Stankiewicz, G. Stefanidis, Complexity and challenges in noncontact high temperature measurements in microwave-assisted catalytic reactors, *Ind. Eng. Chem. Res.* 56 (2017) 13379–13391, <https://doi.org/10.1021/acs.iecr.7b02091>.
- [3] C.O. Kappe, How to measure reaction temperature in microwave-heated transformations, *Chem. Soc. Rev.* 42 (42) (2013) 4977.
- [4] "Ceramics and Composites Processing Methods" Editor(s): Narottam P. Bansal Aldo R. Boccaccini, DOI:10.1002/9781118176665, (2012) *The American Ceramic Society*.
- [5] G. Neuer, G. Jaroma-Weiland, Spectral and total emissivity of high-temperature materials, *Int. J. Thermophys.* 19 (3) (1998) 917–929.
- [6] J. Brübach, C. Pflitsch, A. Dreizler, B. Atakan, On surface temperature measurements with thermographic phosphors: A review, *Prog. Energy Combust. Sci.* 39 (2013) 37–60, <https://doi.org/10.1016/j.pecs.2012.06.001>.
- [7] C. Hsieh, D. Tzou, Z. Huang, C. Lee, J. Chang, High performance infrared heaters using carbon fiber filaments decorated with alumina layer by microwave assisted method, *J. Taiwan Inst. Chem. Eng.* 59 (2016) 521–525.
- [8] P. Honnerová, J. Martan, M. Honner, Uncertainty determination in high-temperature spectral emissivity measurement method of coatings, *Appl. Therm. Eng.* 124 (2017) 261–270, <https://doi.org/10.1016/j.applthermaleng.2017.06.022>.
- [9] G. Neuer and G. Jaroma-Weiland, "Spectral and Total Emissivity of High-Temperature Materials," *International Journal of Thermophysic.I*, vol. 19, no. 3, 1998.
- [10] C. Zhu, M.J. Hobbs, J.R. Willmott, An accurate instrument for emissivity measurements by direct and indirect methods, *Meas. Sci. Technol.* 31 (4) (2020) 044007.
- [11] D. Especel, S. Mattei, Total emissivity measurements without use of an absolute reference, *Infrared Phys. Technol.* 37 (7) (1996) 777–784.
- [12] P. Honnerová, J. Martan, Z. Veselý, M. Honner, Method for emissivity measurement of semitransparent coatings at ambient temperature, *Sci. Rep.* 7 (1) (2017) 1–14.
- [13] E. Copertaro, P. Chiariotti, G.M. Revel, N. Paone, Innovative data regression incorporating deterministic knowledge for soft sensing in the process industry, *J. Process Control* 80 (2019) 180–192, <https://doi.org/10.1016/j.jprocont.2019.06.003>.
- [14] R. Brandt, C. Bird, G. Neuer, Emissivity reference paints for high temperature applications, *Measurement* 41 (2008) 731–736, <https://doi.org/10.1016/j.measurement.2007.10.007>.
- [15] J. Jones, Enhancing the accuracy of advanced high temperature mechanical testing through thermography, *Applied Sciences* 8 (2018) 380, <https://doi.org/10.3390/app8030380>.
- [16] D. Cárdenas-García, Emissivity measurement of high-emissivity black paint at CENAM, *Revista Mexicana de física* 60 (2014) 305–308.
- [17] X. Cheng, W. Duan, W.u. Chen, W. Ye, F. Mao, F. Ye, Q.i. Zhang, Infrared radiation coatings fabricated by plasma spray, *J. Therm. Spray Technol.* 18 (3) (2009) 448–450.
- [18] Z. Liu, Q. Sun, Y. Song, J. Yang, X. Chen, H. Wang, Z. Jiang, High-emissivity composite-oxide fillers for high temperature stable aluminum-chromium phosphate coating, *Surf. Coat. Technol.* 349 (2018) 885–893.
- [19] M. Falz, G. Leonhardt, PVD coatings with high IR emissivity for high temperature applications of Co-based alloys, *Surf. Coat. Technol.* 61 (1–3) (1993) 97–100, [https://doi.org/10.1016/0257-8972\(93\)90209-7](https://doi.org/10.1016/0257-8972(93)90209-7).
- [20] G. Heynderickx, M. Nozawa, High-emissivity coatings on reactor tubes and furnace walls in steam cracking furnaces, *Chem. Eng. Sci.* 59 (2004) 5657–5662, <https://doi.org/10.1016/j.ces.2004.07.075>.
- [21] J. Mao, S. Ding, Y. Li, S. Li, F. Liu, X. Zeng, X. Cheng, Preparation and investigation of MoSi2/SiC coating with high infrared emissivity at high temperature, *Surf. Coat. Technol.* 358 (2019) 873–878.
- [22] H. Luo, X. Zhang, S. Huang, D. Shan, L. Deng, L. He, J. He, Y. Xu, H. Chen, C. Liao, Infrared emissivity and microwave transmission behaviour of flaky aluminium functionalized pyramidal-frustum shaped periodic structure, *Infrared Phys. Technol.* 99 (2019) 123–128, <https://doi.org/10.1016/j.infrared.2019.04.013>.
- [23] X. Guohua, Z. Zuoguang, W. Ruibin, "Matching performance among visible and near infrared coating, low infrared emitting coating and microwave absorbing coating", *Journal of Wuhan Univ. of Tech. – Mater. Sci. Ed.*, Vol 20, No. 4, (2005).
- [24] C. Yan, X. Guo, G. Teng, Z. Ning, Infrared emissivity and microwave absorbing property of epoxy-polyurethane/annealed carbonyl iron composites coatings, *Science China - Technological Sciences* 55 (3) (2012) 623–628, <https://doi.org/10.1007/s11431-011-4696-2>.
- [25] E. Bud Senkowski, "Coatings for Elevated Temperature Service in Process Facilities" *Journal of Protective Coatings & Linings*, 1997, pp: 44-54.

- [26] García-Baños, Beatriz; Catalá Civera, José Manuel; Sánchez-Marín, Juan Rafael; Navarrete Algaba, "High Temperature Dielectric Properties of Iron- and Zinc-Bearing Products during Carbothermic Reduction by Microwave Heating", *Metals*, Vol. 10, 2020.
- [27] B. García-Baños, A.J. Canós, F.L. Penaranda-Foix, J.M. Catalá-Civera, Noninvasive Monitoring of Polymer Curing Reactions by Dielectrometry, *IEEE Sens. J.* 11 (1) (Jan. 2011) 62–70, <https://doi.org/10.1109/JSEN.2010.2050475>.
- [28] J.M. Serra, J.F. Borrás-Morell, B. García-Baños, M. Balaguer, P. Plaza-González, J. Santos-Blasco, D. Catalán-Martínez, L. Navarrete, J.M. Catalá-Civera, Hydrogen production via microwave-induced water splitting at low temperature, *Nat Energy* 5 (2020) 910–919, <https://doi.org/10.1038/s41560-020-00720-6>.
- [29] J.M. Catala-Civera, A.J. Canos, P. Plaza-Gonzalez, J.D. Gutierrez, B. Garcia-Banos, F.L. Penaranda-Foix, Dynamic Measurement of Dielectric Properties of Materials at High Temperature During Microwave Heating in a Dual Mode Cylindrical Cavity, *IEEE Trans. Microw. Theory Tech.* 63 (9) (2015) 2905–2914.
- [30] B. García-Baños, J. Jimenez-Reinosa, F.L. Penaranda-Foix, J.F. Fernandez, J. M. Catalá Civera, Temperature Assessment Of Microwave-Enhanced Heating Processes, *Sci. Rep.* 1 (2019) 1–10.